MAYRA MARTINELLI COSTA

EDUARDA CAROLINE DUARTE AMATTE COELHO

SILVIA FERNANDA MOYA

RAPHAEL SOEIRO SUPPINO

Laboratory of Catalytic Process Engineering and Biorefineries, Department of Process Engineering, School of Chemical Engineering, Universidade Estadual de Campinas (UNICAMP)

INVESTIGATING THE ACIDITY EFFECT OF NIOBIA AS A CATALYTIC SUPPORT FOR FURFURAL CONVERSION

Highlights

- First work in the literature with Ni/Nb_2O_5 as a catalyst for furfural hydrogenation.
- A niobium-based Ni catalyst is an interesting addition to the Brazilian biorefinery portfolio.
- Advantages in catalyst constitution, as Ni is an accessible and inexpensive metal.
- A catalyst predominantly selective to furfuryl alcohol is viable to downstream operations.
- An alternative production process of difurfuryl ether useful to the food industry.

Abstract

As niobia (Nb_2O_5) is an accessible acid support in Brazil, the objective of this work was to evaluate the effect of acidity in Ni/Nb_2O_5 catalysts for the hydrogenation of furfural in the liquid phase. Catalysts with 5, 10, and 15 wt% Ni content were prepared by wet impregnation, activated under H_2 flow, and tested in furfural hydrogenation at 150 °C and 5 MPa of H_2. N_2 physisorption results suggest pore blocking on the support as the amount of Ni increased. The larger crystallites identified by XRD for 15% Ni/Nb_2O_5 probably favored pore blocking, and the atomic composition in EDS versus XPS indicates a lower metallic dispersion for this solid. TPR and XPS results suggest all Ni catalysts are primarily constituted of reduced Ni species, while TPD-NH_3 confirms that the acidity of the support was passed on to the catalysts. The 15 wt% Ni solid led to a slight decrease in activity, which can be related to its lower dispersion. Catalysts proved to be promising in terms of selectivity to furfuryl alcohol, which remained between 60 and 80% throughout the reaction. Also, the acid sites-derived difurfuryl ether was produced with all catalysts and can be an interesting addition to the biorefineries portfolio.

Keywords: Hydrogenation, biorefinery, metallic loading, nickel, niobium oxide, difurfuryl ether.

INTRODUCTION

Considering that fossil resources currently dominate the global supply of energy, chemicals, and materials, greener and renewable alternatives need to be explored. Among many available options, biomass stands out as a readily available source of both fuels and chemicals [1]. Hence the concept of biorefinery arises, as an industry where a cost-effective conversion of biomass yields bioproducts and bioenergy simultaneously, with the aid of optimization strategies related to waste valorization and sustainability [2-4].

There is much potential in the hemicellulosic fraction of biomass. The five-carbon sugar xylose can be obtained from the acid hydrolysis of xylans (hemicellulose constituent) and be further isomerized and dehydrated to form furfural, an essential building block. This is the standard process for furfural production, as the fossil alternative is not economically viable [3,5,6]. Furfural is widely used as a selective organic solvent and has applications in the transportation, pharmaceutical, and agrochemical industries. This product has more than 80 derivatives, including tetrahydrofurfuryl alcohol, 2-methylfuran, and furan, but about 65% of its production is directed toward obtaining furfuryl alcohol [6-10].

The hydrogenation of the aldehyde group in furfural produces furfuryl alcohol, primarily used to produce furan resins, which promotes chemical, thermal, and mechanical stability, as well as resistance to corrosion and solvent act-

ion. However, the industrial process in the gas phase uses a copper-chromite catalyst, an environmentally hazardous solid. Thus, new alternatives have been tested, especially involving supported metal catalysts [6,10,11]. In addition, recent studies have tested the performance of Ni as an active catalyst for furfural conversion in the presence of H_2. The Ni-based catalysts show promising results in terms of activity, with expressive selectivity for hydrogenation, hydrodeoxygenation, decarbonylation, and ring-opening products [12,13]. Figure S1 presents the most common furfural conversion routes and reunites the most important information about furfural and furfuryl alcohol.

Considering the support nature, factors related to availability, sustainability, physicochemical properties, and innovation have been considered. Niobium pentoxide, also known as niobia (Nb_2O_5), can provide high specific surface area and porosity [14], parameters required for catalysis. Moreover, Nb is widely available in Brazil, responsible for about 88% of global niobium production [15]. Nb-based solids such as niobia, niobic acid ($Nb_2O_5.nH_2O$), and niobium phosphate ($NbOPO_4$) are well-established acid catalysts [16], used primarily in reactions that require Brönsted and Lewis acid sites, such as dehydration [17-19]. The catalytic activity of Nb_2O_5 depends on its degree of hydration and the crystalline phase in which the solid is found since it presents polymorphism. For calcination temperatures between 100 and 500 °C, the simultaneous presence of Brönsted and Lewis acid sites can be observed [20], contributing to the acidity of the solid.

Given the above, this research aims to evaluate the acidity effect of Nb_2O_5 as a catalytic support for furfural hydrogenation in the liquid phase. It is noteworthy that the use of niobia in this reaction system still has not been largely explored in the literature, hence evaluating a low-cost catalyst such as Ni/Nb_2O_5 for possible application in biorefinery processes constitutes the main contribution of this work.

EXPERIMENTAL

Catalyst preparation

Catalysts comprising Ni supported on Nb_2O_5 ($Nb_2O_5.nH_2O$, supplied by the Brazilian Metallurgy and Mining Company, CBMM) were synthesized by wet impregnation, following the method described by Suppino *et al.* [21,22]. Nickel chloride, $NiCl_2$ (Sigma Aldrich, 98% purity), was chosen as the metal precursor. Ni loading was tested as 5, 10, and 15 wt% in an attempt to boost the performance of this non-noble metal and investigate the influence of this parameter.

Niobia was synthesized via calcination of niobic acid with synthetic air (80 mL/min) at 400 °C for 4 hours. The wet impregnation was performed by slowly adding the water-diluted precursor to a suspension containing the support. The suspension was heated to 80 °C, and its pH was adjusted to 7 by the addition of NH_4OH (0.5 mol/L) to be above the point of zero charge of the support (~pH 4), obtained via potentiometric titration and in accordance to Kosmulski [23]. After pH adjustment and filtration, solids were washed with deionized water until chlorine was no

longer identified in the $AgNO_3$ test. The reduction was accomplished under 60 mL/min H_2 flow, at 400 °C, for 3 hours. To minimize metal oxidation, catalysts were kept under an Ar atmosphere to form a protective layer of inert gas above the materials' surface [21,22].

Support and catalysts characterization

The solids were characterized by N_2 physisorption using models BET and BJH, to obtain information about their textural properties. The analyses were performed at -196 °C in a Tristar Micromeritics equipment (model ASAP 2010). Samples were previously pretreated under vacuum at 200 °C for 12 hours. In all BET graphs, the coefficient of determination was $R^2 > 0,999$, which indicates an adequate adjustment of the model.

The elemental composition of the solids was semi-quantitatively evaluated by scanning electronic microscopy coupled with spectrometric X-ray analysis (SEM/EDS). The analyses were performed in a LEO Electron microscope (model LEO 440i). For SEM, the conditions applied were an electrical current of 100 pA and 20 kV, with 25 mm focus (magnification 1000x). Meanwhile, EDS was based on elemental mapping, with a 70 eV system resolution, using the ZAF method with 4 to 5 interactions.

The crystalline phases of catalysts were investigated with X-ray diffraction (XRD). The analyses were carried out in a Phillips Analytical X-Ray equipment (model X'Pert-MPD). The applied conditions were: 2θ from 20° to 80°, 0.02° step, 40 kV voltage, 40 mA current, 0.04°/s scanning, and 0.5 s/step. It is possible to estimate the mean crystallite size (s) using the Scherrer Equation. For spherical crystallites, the characteristic constant K is often 0.9 [24].

X-ray photoelectron spectroscopy (XPS) was applied to analyze the surface composition and the oxidation states of the active phase, using a spherical analyzer VSWHA-100 with an aluminum anode (Al Kα, hν = 1486.6 eV). The pressure achieved was lower than 2.10^{-12} MPa. To correct the binding energies, line C 1s with a binding energy of 284.6 eV was considered for reference.

The profile corresponding to the degree of reduction of previously reduced catalysts was studied with temperature-programmed reduction (TPR) in a Micromeritics AutoChem 2910 equipment. In TPR, solids were heated under 60 mL/min flow of a 10% H_2/Ar mixture, with a heating rate of 10 °C/min, from 25 °C to 600 °C. The total time of analysis was around 60 min. The degree of reduction was estimated by a ratio between the values of actual and nominal H_2 consumption, subtracted from 1 (100%).

Temperature-programmed desorption using NH_3 as a basic probe molecule (TPD-NH_3) was also performed in a Micromeritics AutoChem 2910 equipment containing a TCD detector, to study the acidity of the solids. Pretreatment was accomplished with 25 mL/min He flow at 300 °C (10 °C/min). Saturation was conducted under 25 mL/min NH_3 flow (30% NH_3 and 70% He) for 30 minutes at 50 °C. Samples were flushed with He also for 30 minutes at 50 °C to remove the physisorbed NH_3. Finally, samples were heated to 500 °C (10 °C/min) and this temperature was kept for 20 minutes. The total time of analysis was around 65 minutes.

Catalytic tests

All chemical reagents used in catalytic tests were supplied by Sigma Aldrich, with purity higher than 98%. Catalysts were externally reduced under H_2 flow before reactions, as described in the Experimental section.

Catalytic tests were carried out in a slurry Parr reactor of 300 mL capacity initially filled with 300 mg of Ni catalyst, 38.9 g of 2-propanol, chosen as the solvent, and 2.1 g of heptane, used as an internal standard for chromatographic quantification. The reactor was hermetically closed, purged with N_2 three times, and subsequently pressurized to 5 MPa of H_2 with agitation adjusted to 1000 rpm. When a reaction temperature of 150 °C was reached, 8.7 g of furfural was added directly to the reactor through an ampoule, to obtain a substrate concentration of 1.5 mol/L.

Reactants and products were quantified in an HP-5890 series II gas chromatograph equipped with a flame ionization detector (FID). A calibration curve was constructed with the internal standard. The injection in triplicate suggests a standard deviation below 5%. An OV-5 capillary column was used, with 5% diphenyl and 95% dimethylpolysiloxane stationary phase. Samples collected at the end of the reaction (5 hours) were also submitted to gas chromatography coupled with mass spectrometry (GC-MS) using a Perkin Elmer equipment (GC: AutoSystem XL and MS: TurboMass). Similar analytical conditions were applied, with an NST-5 capillary column.

The conversion was calculated as moles of furfural reacted divided by moles of furfural at the beginning of the reaction. Selectivity was calculated as the mole percentage of a specific product relative to all identified liquid products.

RESULTS AND DISCUSSION

Characterization results

Table 1 presents the results of metal content, specific surface area, mean pore diameter, and crystalline domain size. There is an agreement between the nominal metal loading of the solids and the results given by the EDS analysis. No signs of residual chlorine were identified. Additionally, the SEM images in Figure S2 show no modifications related to morphology after metallic impregnation.

The isotherms obtained by N_2 physisorption are present in Figure S3. The support and Ni catalysts possess type IV(a) isotherms which correspond to mesoporous solids [25]. The Nb_2O_5 support has a specific surface area of 126 m^2/g, which agrees with previously reported values for Nb_2O_5 calcined at 400 °C [26,27]. The impregnation of Ni on the surface of niobia did not affect the total pore volume; however, there was a slight but gradual decrease in the specific surface area of the catalysts, if compared to the support (up to 30% for 15%/Nb_2O_5). Also, an increase in the mean pore diameter of supported catalysts was noticed with the increase in Ni loading. These findings suggest the occurrence of a partial pore blockage on the support, more significant as the amount of impregnated Ni increased.

Figure 1 contains the XRD diffractograms for the calcined support, as well as for the Ni-reduced catalysts.

The XRD results indicate the presence of a predominantly non-crystalline structure for the support. Otherwise, it is observed some crystallinity degree by the Ni metallic phase for the three catalysts. Peaks corresponding to metallic Ni (JCPDS 01-070-1849) were identified, leading to the conclusion that at least some degree of reduction was achieved at 400 °C and pure H_2 gas. As shown in Table 1, the solid containing 15 wt% Ni has the largest mean Ni crystallite size (32 nm). Therefore, the larger crystallites likely favored pore blocking.

As for the TPR results, values of peak temperature and degree of reduction are reported in Table 2, while the H_2 consumption profiles for previously reduced catalysts are present in Figure 2. It is essential to highlight that the TPR was performed to evaluate the efficiency of the reduction method and how much of the metallic phase would remain on the surface after catalysts were exposed to the atmosphere. The profile corresponding to the support is also shown, which is proved irreducible under the conditions applied.

The H_2 consumption peaks identified in TPR at a temperature range of 150-200 °C are probably due to the oxidation of Ni in the form of Ni(II), which is typical for non-noble catalysts exposed to atmospheric conditions [28]. Surface reoxidation in this temperature range has been reported elsewhere [29,30]. Considering this hypothesis, all Ni catalysts present a degree of reduction higher than 95%, which confirms that the reduction was appropriate and effective and that the atmospheric exposure led to significant oxidation for none of the catalysts.

As for the XPS results, Table 3 shows the binding energies of the peaks found in each spectrum and the probable surface composition of the catalysts. To verify that the metallic active phase for hydrogenation is indeed on the surface, there is also a comparison between the Ni/Nb atomic ratios measured through XPS and EDS. Figure 3 presents the XPS spectra for the 5, 10, and 15 wt% Ni catalysts.

Peaks around 852 eV and 855 eV were commonly observed for Ni catalysts. The binding energy of 852 eV corresponds to Ni(0) while the peak in 855 eV can be attributed to Ni(II) [31], which has also been reported for other Ni catalysts reduced by H_2 flow at 400 °C [30]. Therefore, the TPR and XPS results suggest that all three Ni catalysts are primarily constituted of reduced Ni species, with a partially oxidized surface of a few atomic layers depth.

Another possible analysis of the surface properties can be accomplished by comparing the atomic composition using the ratio Ni/Nb, which indicates an enrichment of Ni over the surface when compared with the bulk composition for all catalysts. However, the difference between the ratios is less pronounced for the 15 wt% Ni solid. This solid presented an increase of 78% in its mean crystallite size, compared to 10% Ni/Nb_2O_5, therefore it is expected that the metal dispersion on the surface has been compromised.

Table 4 shows the TPD-NH_3 results, while Figure 4 displays the profiles obtained in the analyses for the support and catalysts. The support presents a total acidy of 676 µmol NH_3/g, primarily including weak and medium-

strength acid sites [32]. This TPD profile is consistent with previous studies with calcined Nb_2O_5, also provided by CBMM [17,33]. The acidity values tend to drop with the increase of calcination temperature, once the crystalline transition causes suppression of acid sites [20]. Therefore, the acidity values found for niobia calcined at 300 °C [33], 400 °C (this work), and 500 °C [17] decrease with calcination temperature, as expected.

Table 1. Ni loading obtained by EDS, textural features obtained by N_2 physisorption, and mean Ni crystallite size obtained by XRD using the Scherrer Equation.

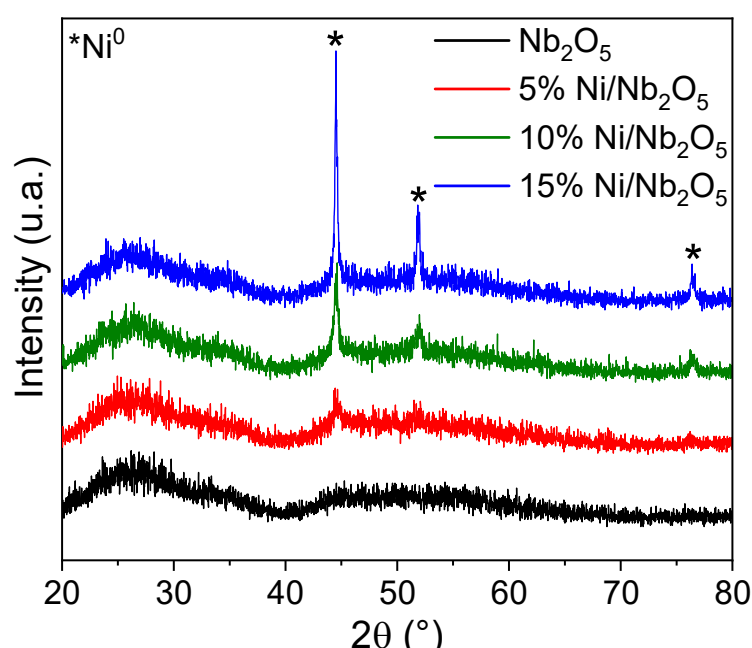| Material	% Ni (w/w)	Specific surface area (m^2/g)	Mean pore diameter (nm)	Ni (111) mean crystallite size (nm)
Nb_2O_5	---	126	5.7	---
5% Ni/Nb_2O_5	5	111	6.7	17
10% Ni/Nb_2O_5	10	104	7.0	18
15% Ni/Nb_2O_5	14	89	7.5	32

Figure 1. XRD diffractograms for Nb_2O_5 and catalysts containing 5, 10, and 15% Ni/Nb_2O_5.

Table 2. Peak temperature and degree of reduction obtained by TPR.

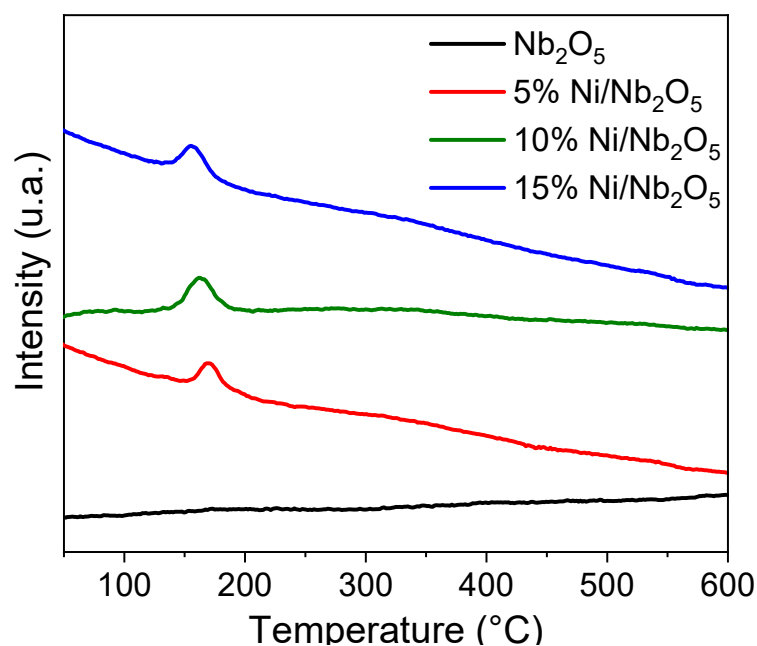| Material	Peak temperature (°C)	Degree of reduction (%)
Nb_2O_5	---	---
5% Ni/Nb_2O_5	170	95
10% Ni/Nb_2O_5	161	95
15% Ni/Nb_2O_5	157	98

Figure 2. TPR profiles for Nb_2O_5 and previously reduced 5, 10, and 15% Ni/Nb_2O_5 catalysts.

Table 3. Surface composition obtained by XPS and comparison of the Ni/Nb atomic ratio in XPS and EDS.

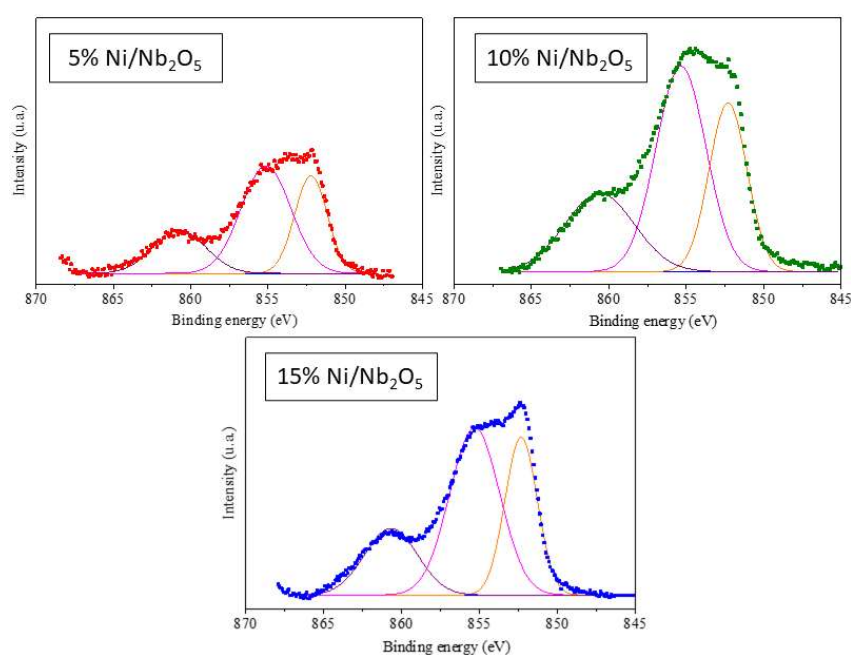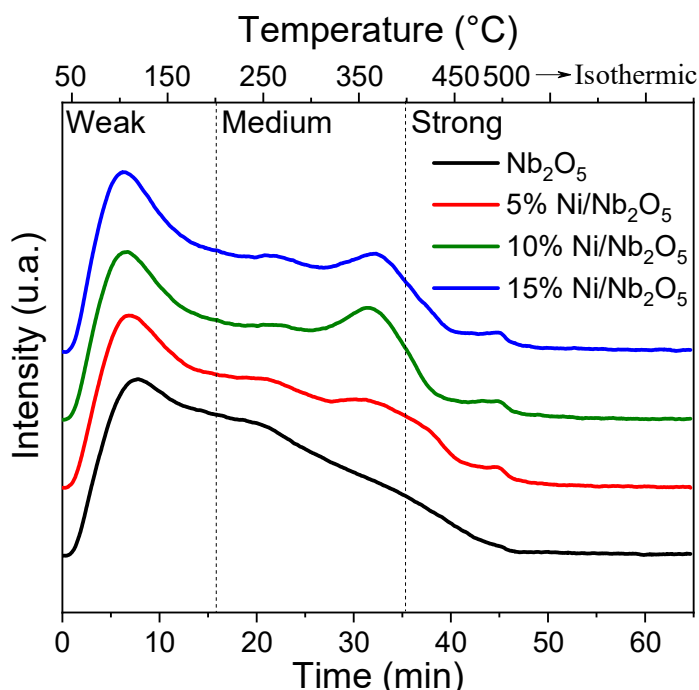| Material	Binding Energy (eV)	Probable species on the surface	Ni/Nb atomic ratio in XPS	Ni/Nb atomic ratio in EDS
5% Ni/Nb_2O_5	852.2 855.1 860.7	Ni(0) Ni(II) satellite peak	0.23	0.13
10% Ni/Nb_2O_5	852.3 855.3 860.6	Ni(0) Ni(II) satellite peak	0.93	0.31
15% Ni/Nb_2O_5	852.3 855.3 860.7	Ni(0) Ni(II) satellite peak	0.50	0.41

Figure 3. XPS spectra for 5, 10, and 15% Ni/Nb_2O_5.

Table 4. Total acidity and acid site density obtained by TPD-NH₃.

Material	Total acidity ($\mu mol_{NH3}/g$)	Acid sites density ($\mu mol_{NH3}/m^2$)
Nb_2O_5	676	5.4
5% Ni/Nb_2O_5	619	5.6
10% Ni/Nb_2O_5	673	6.5
15% Ni/Nb_2O_5	593	6.7

Figure 4. TPD-NH₃ profiles for Nb₂O₅ and catalysts containing 5, 10, and 15% Ni/Nb₂O₅.

In terms of total acidity, there has been little change between the support and the Ni catalysts, with a maximum decrease of 12%. As observed in Table 1, the specific surface area of the catalysts was gradually reduced as the Ni loading increased, resulting in an increase in acid site density with the increment in metal content. A peak near 400 °C, observed for all Ni-supported catalysts, reflects differences in their acidity compared to the support.

According to Guo and Zaera [34], oxygen species originating from partially oxidized surfaces can act as Lewis acid sites for NH_3 adsorption. As discussed earlier in this work, the presence of partially oxidized Ni over the surface was detected for all catalysts.

The TPD-NH₃ results display similarities in acidity for all evaluated materials, which suggests that metallic impregnation, calcination, and reduction thermal treatments did not significantly alter the natural acidity of the support. Therefore, the presence of acidity in the metal-supported catalysts makes them bifunctional, capable of promoting not only hydrogenation to furfuryl alcohol but also other reactions that take place in acid sites [35].

Reaction results

Before discussing the results obtained with Ni as the active phase, it is important to mention that a control reaction was performed using only the calcined support (Nb_2O_5) as a catalyst. After 5h, less than 5% conversion was obtained, with traces of furfuryl alcohol identified. Thus, the support could not hydrogenate furfural on its own, and a metallic active phase is needed in this case. Moreover, the presence of acid sites in niobia might have led to the transformation of furfuryl alcohol to difurfuryl ether, as traces of this last compound were found. This result is an illustration of the acidic characteristic of the support, as it seems to be active for this dehydration reaction.

Another important detail is that, in the reactions of this research, the solvent 2-propanol did not act as an H_2 donor in a Meerwein-Ponndorf-Verley mechanism (MPV), as observed by Li *et al.* [36]. Typical products of 2-propanol decomposition, such as acetone and isopropyl ethers, were not identified in the chromatograms, so the H_2 consumed in the reactions came exclusively from the high-pressure atmosphere created in the reactor.

Figure 5 presents the furfural conversion profile, while Figure 6 presents selectivity to furfuryl alcohol and difurfuryl ether throughout the reactions, with 5, 10, and 15 wt% Ni catalysts. A similar performance was observed with all three solids, with a gradual increase of furfural conversion over time achieving 39, 47, and 41% after 5 h for 5, 10, and

15% Ni/Nb_2O_5, respectively. Despite containing a greater amount of impregnated Ni, which is the active phase responsible for hydrogenation, 15% Ni/Nb_2O_5 presented a slight decrease in catalytic activity. This behavior can be related to a lower metallic dispersion in this catalyst, as suggested by the largest mean crystallite size, 32 nm (XRD result, Table 1), and also by the value encountered for Ni/Nb atomic ratio (XPS result, Table 3), which can lead to a decrease of potential active sites on the surface.
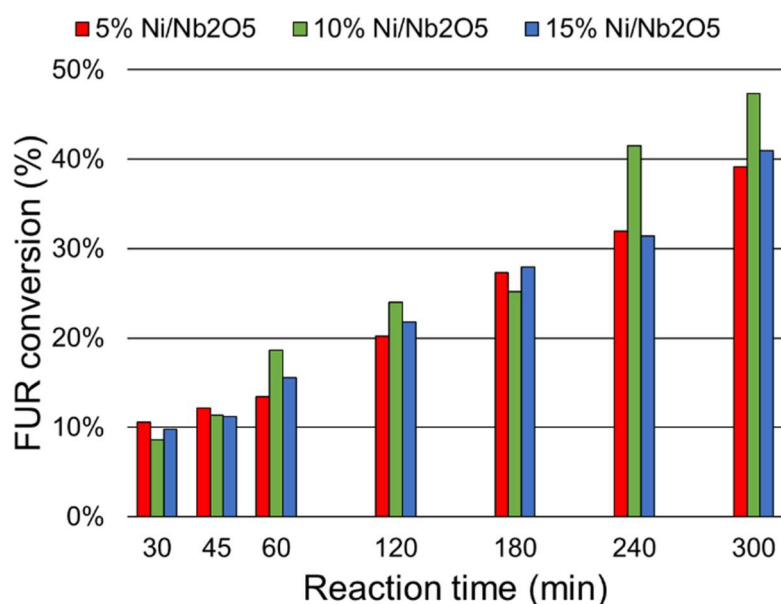

Figure 5. Conversion of furfural measured throughout the reactions catalyzed by 5, 10, and 15% Ni/Nb_2O_5. Reaction conditions: 5 MPa of H_2, 150 °C, agitation speed of 1000 rpm, 300 mg of catalyst.
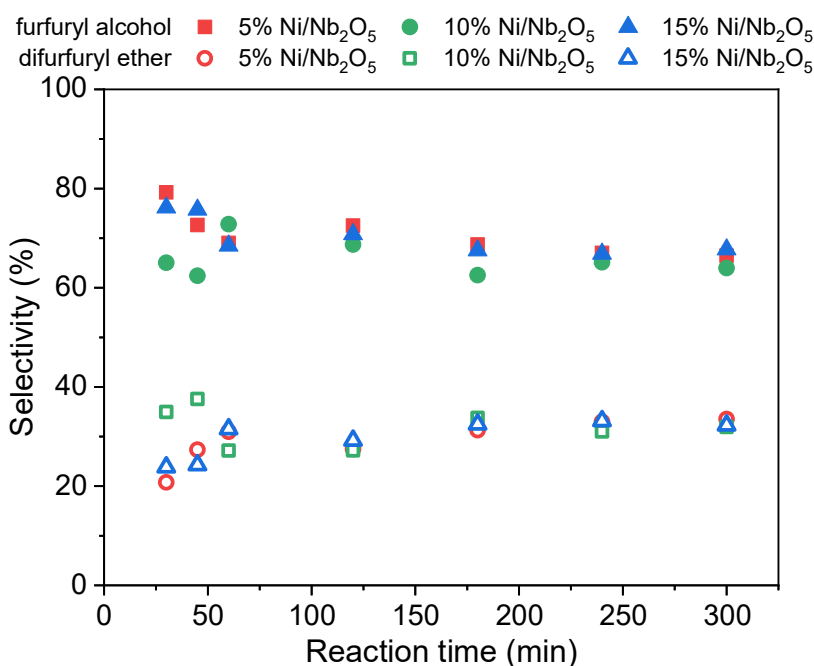

Figure 6. Selectivity to furfuryl alcohol and difurfuryl ether measured throughout the reactions catalyzed by 5, 10, and 15% Ni/Nb_2O_5. Reaction conditions: 5 MPa of H_2, 150 °C, agitation speed of 1000 rpm, 300 mg of catalyst.

Despite the loss in activity with the increase of Ni loading, it is vital to highlight the selectivity tendency that all three solids have presented. Figure 6 shows that the selectivity to furfuryl alcohol remains roughly between 60% and 80% throughout the reaction time for all Ni catalysts. Although these catalysts can be considered bifunctional, as they retained the acidity of the support, the main reaction product was furfuryl alcohol.

The selectivity results are of great interest, as furfural in the presence of H_2 can originate other products, as seen in Figure S1. Table S1 presents Ni catalysts used in furfural hydrogenation to furfuryl alcohol previously reported in the

literature. These catalysts were tested in liquid batch reactions, in experimental conditions similar to this work (synthesis, activation, reaction).

Among all previous applications of Ni in furfural conversion, only 18 were selected according to the criteria previously described, which proves that it is hard to obtain high selectivity to furfuryl alcohol with Ni as the active phase. Even so, Ni/Nb_2O_5 catalysts in this research presents selectivity to furfuryl alcohol comparable to the best results reported in the literature.

Considering this work was exploratory - an introduction of a new catalyst in a selected reaction system - there was no attempt to optimize the catalytic activity. In turn, since the potential of Ni/Nb_2O_5 to produce furfuryl alcohol has been proven, it is now possible to optimize reaction parameters in future research.

The GC-MS analyses were carried out to identify by-products possibly correlated to the nature of the support. The results suggest the presence of difurfuryl ether, with selectivity values of 20-40% throughout the reaction. In the presence of bifunctional catalyst Ni/Nb_2O_5, furfural was firstly hydrogenated to furfuryl alcohol in metallic sites, followed by etherification in acid sites, as also reported elsewhere [37-39]. Difurfuryl ether is widely applied in the food industry as a flavoring agent, and its most common synthesis route is a two-step process of bromination followed by etherification, which is known as environmentally hazardous, so new alternative processes need to be explored [40].

A catalyst recycling test was performed to assess catalyst reusability, and a new set of reactions was carried out with the 10 wt% Ni catalyst, in the same conditions. This catalyst was chosen for the reusability tests due to the higher results in converting furfural on the fresh test (47%). On its second use, a conversion of 42% was obtained, practically repeating the performance of the fresh catalyst. However, in the third cycle, the activity dropped considerably (17%). It is noteworthy that the catalyst was not submitted to any sort of treatment before its reuse, which could restore most of its activity. A more future study, regarding the deactivation mechanism and potential regeneration is required to fully assess these results. Nevertheless, the catalyst was able to maintain the same selectivity profile in all three reactions, with nearly no loss in the production of furfuryl alcohol and difurfuryl ether. The results can be found in Figure S4 (conversion) and Figure S5 (selectivity).

To investigate whether selectivity would be maintained for a long time, catalyst 10% Ni/Nb_2O_5 was tested in a 10-hour reaction. Apparently, this is a system with steady selectivity, regardless of the time frame or catalytic cycle. It is worth mentioning that the conversion profile resembles a second-degree polynomial and tends to stabilize around ten hours, at approximately 55% furfural conversion. Nevertheless, doubling the reaction time has only increased furfural conversion in ca. 5%, which could not be a feasible aspect considering a future industrial application of this catalyst. Modifications in catalytic synthesis or reaction conditions should be performed to achieve higher conversions and this is a topic for future research. The results are presented in Figure S6 (conversion) and Figure S7 (selectivity).

In summary, the Ni/Nb_2O_5 studied in this work was found to be predominantly selective to furfuryl alcohol, currently the most important furfural derivative. As selectivity is a crucial parameter to the viability of a production process, especially in terms of downstream operations, this reaction system has the potential to be integrated into biorefineries. There are also many advantages in terms of catalyst constitution, as a simple synthesis and activation procedure is proposed, and Ni is an accessible and inexpensive metal. Also, the use of niobia as catalytic support for furfural hydrogenation is still incipient, and this work is the first report with Ni-supported catalysts in this reaction. As niobium is a strategic asset for Brazil, a niobium-based Ni catalyst could be an interesting addition to the Brazilian biorefinery portfolio. Furthermore, the findings of this work provide an alternative production process of difurfuryl ether that can also benefit the food industry.

CONCLUSION

The present work was conceived from the question: what would be the influence of niobia as support in Ni catalysts for the hydrogenation of furfural? From there, a series of developments emerged. However, it is believed that the central question has been answered: Ni/Nb_2O_5 catalysts are capable of hydrogenating furfural to furfuryl alcohol, with the direct influence of metallic loading, whereas the acidity of the support also plays a crucial role in the reaction, as difurfuryl ether was found in the reaction medium.

The results obtained can be considered promising. In the reaction conditions applied in this work, catalysts were able to maintain a high and steady selectivity to furfuryl alcohol for at least ten hours. However, the increase of Ni loading from 10 to 15 wt% did not lead to a higher catalyst activity, probably due to an impaired dispersion of Ni on the surface. All in all, a steady selectivity is ideal for industrial processes, and due to its high availability in Brazil, expanding the knowledge about niobium applications can lead to significant economic and technological advances for our country.

REFERENCES

[1] I. Ahmed, M.A. Zia, H. Afzal, S. Ahmed, M. Ahmad, Z. Akram, F. Sher, H.M.N. Iqbal, Sustainability (Switzerland) 13 (2021) 1-32. https://doi.org/10.3390/su13084200.

[2] S.S. Hassan, G.A. Williams, A.K. Jaiswal, Renewable Sustainable Energy Rev. 101 (2019) 590-599. https://doi.org/10.1016/j.rser.2018.11.041.

[3] B. Kumar, P. Verma, Fuel 288 (2021) 119622. https://doi.org/10.1016/j.fuel.2020.119622.

[4] E. Scopel, C.A. Rezende, Ind. Crops. Prod. 163 (2021) 113336. https://doi.org/10.1016/j.indcrop.2021.113336.

[5] C.B.T.L. Lee, T.Y. Wu, Renewable Sustainable Energy Rev. 137 (2021) 110172. https://doi.org/10.1016/j.rser.2020.110172.

[6] R. Mariscal, P. Maireles-Torres, M. Ojeda, I. Sádaba, M. López Granados, Energy Environ. Sci. 9 (2016) 1144-1189. https://doi.org/10.1039/C5EE02666K.

[7] M. Ghashghaee, S. Shirvani, V. Farzaneh, S. Sadjadi, Braz. J. Chem. Eng. 35 (2018) 669-678. https://doi.org/10.1590/0104-6632.20180352s20160703.

[8] J.F.L. Silva, M.A. Selicani, T.L. Junqueira, B.C. Klein, S. Vaz Júnior, A. Bonomi, Braz. J. Chem. Eng. 34 (2017) 623-634. https://doi.org/10.1590/0104-6632.20170343s20150643.

[9] M.L. Testa, M.L. Tummino, Catalysts 11 (2021) 1-27. https://doi.org/10.3390/catal11010125.

[10] K. Yan, G. Wu, T. Lafleur, C. Jarvis, Renewable Sustainable Energy Rev. 38 (2014) 663-676. https://doi.org/10.1016/J.RSER.2014.07.003.

[11] P. Khemthong, C. Yimsukanan, T. Narkkun, A. Srifa, T. Witoon, S. Pongchaiphol, S. Kiatphuengporn, K. Faungnawakij, Biomass Bioenergy 148 (2021) 106033. https://doi.org/10.1016/j.biombioe.2021.106033.

[12] H. Tian, G. Gao, Q. Xu, Z. Gao, S. Zhang, G. Hu, L. Xu, X. Hu, Mol. Catal. 510 (2021) 111697. https://doi.org/10.1016/j.mcat.2021.111697.

[13] Z. Zhang, K. Sun, Y. Ma, Q. Liu, Q. Li, S. Zhang, Y. Wang, Q. Liu, D. Dong, X. Hu, Catal. Sci. Technol. 9 (2019) 4510-4514. https://doi.org/10.1039/c9cy00985j.

[14] A. Florentino, P. Cartraud, P. Magnoux, M. Guisnet, Appl. Catal., A 89 (1992) 143-153. https://doi.org/10.1016/0926-860X(92)80229-6.

[15] U.S. Geological Survey, Mineral Commodity Summaries, Virginia (2019). https://doi.org/10.3133/70202434.

[16] S. Kang, R. Miao, J. Guo, J. Fu, Catal. Today 374 (2021) 61-76. https://doi.org/10.1016/j.cattod.2020.10.029.

[17] L.F. de Lima, J.L.M. Lima, D.S.S. Jorqueira, R. Landers, S.F. Moya, R.S. Suppino, React. Kinet., Mech. Catal. 132 (2021) 73-92. https://doi.org/10.1007/s11144-021-01931-y.

[18] K. Skrodczky, M.M. Antunes, X. Han, S. Santangelo, G. Scholz, A.A. Valente, N. Pinna, P.A. Russo, Commun. Chem. 2 (2019) 1-11. https://doi.org/10.1038/s42004-019-0231-3.

[19] J.L. Vieira, G. Paul, G.D. Iga, N.M. Cabral, J.M.C. Bueno, C. Bisio, J.M.R. Gallo, Appl. Catal., A 617 (2021) 118099. https://doi.org/10.1016/j.apcata.2021.118099.

[20] T. Iizuka, K. Ogasawara, K. Tanabe, Bull. Chem. Soc. Jpn. 56 (1983) 2927-2931. https://doi.org/10.1246/bcsj.56.2927.

[21] R.S. Suppino, R. Landers, A.J.G. Cobo, Appl. Catal., A 452 (2013) 9-16. https://doi.org/10.1016/j.apcata.2012.11.034.

[22] R.S. Suppino, R. Landers, A.J.G. Cobo, Appl. Catal., A 525 (2016) 41-49. https://doi.org/10.1016/j.apcata.2016.06.038.

[23] M. Kosmulski, Adv. Colloid Interface Sci. 238 (2016) 1-61. https://doi.org/10.1016/j.cis.2016.10.005.

[24] G. Ertl, H. Knözinger, F. Schüth, Handbook of heterogeneous catalysis, Wiley-VCH, Weinheim (2008).

[25] M. Thommes, K. Kaneko, A.V. Neimark, J.P. Olivier, F. Rodriguez-Reinoso, J. Rouquerol, K.S.W. Sing, Pure Appl. Chem. 87 (2015) 1051-1069. https://doi.org/10.1515/pac-2014-1117.

[26] R. Brayner, F. Bozon-Verduraz, Phys. Chem. Chem. Phys. 5 (2003) 1457-1466. https://doi.org/10.1039/b210055j.

[27] K.M.A. Santos, E.M. Albuquerque, L.E.P. Borges, M.A. Fraga, Mol. Catal. 458 (2018) 198-205. https://doi. org/10.1016/j.mcat.2017.12.010

[28] F. Huber, Z. Yu, S. Lögdberg, M. Rønning, D. Chen, H. Venvik, A. Holmen, Catal. Lett. 110 (2006) 211-220. https://doi.org/10.1007/s10562-006-0111-1.

[29] R.S. Suppino, R. Landers, A.J.G. Cobo, React. Kinet. Mech. Catal. 114 (2015) 295-309. https://doi.org/10.1007/s11144-014-0790-3.

[30] S. Jantarang, E.C. Lovell, T.H. Tan, J. Scott, R. Amal, Prog. Nat. Sci.: Mater. Int. 28 (2018) 168-177. https://doi.org/10.1016/j.pnsc.2018.02.004.

[31] National Institute of Standards and Technology, NIST X-ray Photoelectron Spectroscopy Database, NIST Standard Reference Database Number 20 (2012). https://doi.org/10.18434/T4T88K

[32] P. Berteau, B. Delmon, Catal. Today 5 (1989) 121-137. https://doi.org/10.1016/0920-5861(89)80020-3.

[33] V.M. Benitez, S.P. de Lima, M. do Carmo Rangel, D. Ruiz, P. Reyes, C.L. Pieck, Catal. Today 289 (2017) 53-61. https://doi.org/10.1016/j.cattod.2016.10.004.

[34] H. Guo, F. Zaera, Surf. Sci. 524 (2003) 1-14. https://doi.org/10.1016/S0039-6028(02)02486-X.

[35] A.M. Robinson, J.E. Hensley, J.W. Medlin, ACS Catal. 6 (2016) 5026-5043. https://doi.org/10.1021/acscatal.6b00923.

[36] F. Li, W. Zhu, S. Jiang, Y. Wang, H. Song, C. Li, Int. J. Hydrogen Energy 45 (2019) 1981-1990. https://doi.org/10.1016/j.ijhydene.2019.11.139.

[37] A. Aldureid, F. Medina, G.S. Patience, D. Montané, Catalysts 12 (2022) 390. https://doi.org/10.3390/catal12040390.

[38] M.A. Jackson, M.G. White, R.T. Haasch, S.C. Peterson, J.A. Blackburn, Mol. Catal. 445 (2018) 124-132. https://doi.org/10.1016/j.mcat.2017.11.023.

[39] Á. O'Driscoll, J.J. Leahy, T. Curtin, Catal. Today 279 (2017) 194-201. https://doi.org/10.1016/j.cattod.2016.06.013.

[40] S. Yang, Y. Hao, J. Wang, H. Wang, Y. Zheng, H. Tian, Sci. Rep. 7 (2017) 12954. https://doi.org/10.1038/s41598-017-13472-3.

MAYRA MARTINELLI COSTA

EDUARDA CAROLINE DUARTE AMATTE COELHO

SILVIA FERNANDA MOYA

RAPHAEL SOEIRO SUPPINO

Laboratory of Catalytic Process Engineering and Biorefineries, Department of Process Engineering, School of Chemical Engineering, Universidade Estadual de Campinas (UNICAMP)

NAUČNI RAD

ISTRAŽIVANJE EFEKTA KISELOSTI NIOBIJUM-PENTAOKSIDA KAO NOSAČA KATALITIZATORA KONVERZIJU FURFURALA

Pošto je niobijum-pentaoksid (Nb_2O_5) pristupačan kiseli nosač u Brazilu, cilj ovog rada je bio da se proceni efekat kiselosti Ni/Nb_2O_5 katalizatora za hidrogenaciju furfurala u tečnoj fazi. Katalizatori sa 5, 10 i 15% Ni su pripremljeni vlažnom impregnacijom, aktivirani u struji H_2 i testirani u hidrogenaciji furfurala na 150 °C i 5 MPa H_2. Rezultati fizisorpcije N_2 ukazuju na blokiranje pora na nosaču sa povećanjem količine Ni. Veći kristaliti identifikovani XRD-om za 15% Ni/Nb_2O_5 verovatno su favorizovali blokiranje pora, a atomski sastav određen EDS-om u odnosu na sastav određen XPS-om ukazuje na manju disperziju metala za ovu čvrstu supstancu. Rezultati TPR i XPS ukazuju na to da su svi Ni katalizatori prvenstveno sastavljeni od redukovanih Ni vrsta, dok TPD-NH_3 potvrđuje da je kiselost nosača preneta na katalizatore. Čvrsta supstanca Ni sa 15% dovela je do blagog smanjenja aktivnosti, što se može povezati sa njenom manjom disperzijom. Katalizatori su se pokazali obećavajućim u selektivnosti prema furfuril-alkoholu, koji je ostao između 60 i 80% tokom cele reakcije. Takođe, difurfuril-etar dobijen iz kiselih mesta je proizveden sa svim katalizatorima i može biti zanimljiv dodatak portfoliju biorafinerija.

Ključne reči: Hidrogenacija, biorafinerija, metalno punjenje, nikl, niobijum oksid, difurfuril etar.